STARK BROADENING OF Co II SPECTRAL LINES FOR STELLAR SPECTRA INVESTIGATIONS

ZLATKO MAJLINGER[1,2] MILAN S. DIMITRIJEVIĆ[1],
AND VLADIMIR A. SREĆKOVIĆ[2]

[1]Astronomical Observatory, Volgina 7, 11060 Belgrade 38, Serbia

[2] Department of Physics, Faculty of Science, University of Zagreb, Bijenička cesta 32, 10000 Zagreb, Croatia

[3]Institute of Physics Belgrade, University of Belgrade, Pregrevica 118, 11080 Belgrade, Serbia

Abstract

In this contribution Stark Full Widths at Half Maximum for 46 Co II multiplets have been calculated (Majlinger et al., 2018, 2020a) by modified semiempirical method described in Dimitrijević and Konjević, (1980).The calculated results have been used to investigate the importance of Stark broadening mechanism for CoII lines in A type star and DA and DB white dwarf atmospheres (Majlinger et al., 2020a, b). Stark broadening parameters from this paper will enter in the STARK-B database (http://stark-b.obspm.fr/).

Introduction

Stark Full Widths at Half Maximum for 46 Co II multiplets have been calculated (Majlinger et al., 2018, 2020a) using modified semiempirical method (Dimitrijević and Konjević, 1980). The obtained results (Tab 1,2) have been used to investigate the significance of Stark broadening mechanism for Co II lines in DA and DB white dwarf (WD) and A type star atmospheres. We examined the influence of surface gravity (log g), effective temperature and wavelength of the spectral line, on the importance of the inclusion of Stark broadening contribution in the profiles of the considered Co II spectral lines, for plasma conditions in atmospheric layers corresponding to different stellar opacities. For the purpose of this work, we choose four lines from the list of 46 Co II spectral lines for which Stark widths have already been calculated and published elsewhere (Majlinger et al., 2018, 2020a) and we investigated if possible domination of Stark broadening under the Doppler broadening for each of these four lines exists (Majlinger et al, 2020b). To show this, the different models of atmosphere of A-type star (Kurucz, 1979) and DA and DB WD (Wickramarsinghe, 1972, Koester, 1980) are used. Stark and Doppler broadening is presented as a function of optical depth or temperature of atmospheric layers (Figs 1-9).

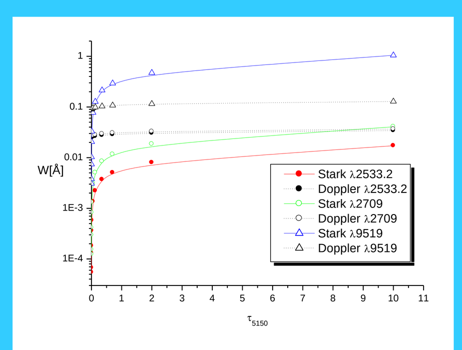

Fig. 1. Stark and Doppler broadening for spectral lines λ2533.2, λ2709, and λ9519 as a function of optical depth in the atmosphere of DA white dwarf (Majlinger et al, 2020a). Simulation is done with choice of model parameters T_{eff} = 15000 K and log g = 8 (Wickramarsinge, 1972).

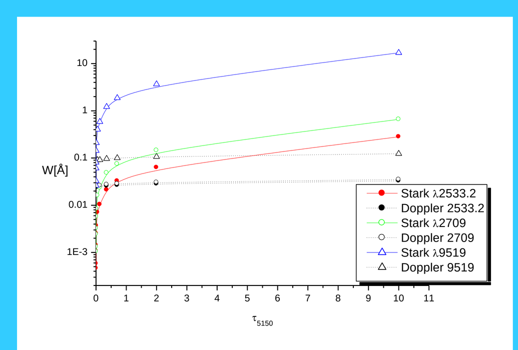

Fig. 2. Stark and Doppler broadening for spectral lines λ2533.2, λ2709, and λ9519 as a function of optical depth in the atmosphere of DB white dwarf (Majlinger et al, 2020a). Simulation is done with choice of the same model parameters, T_{eff} = 15000 K and log g = 8.

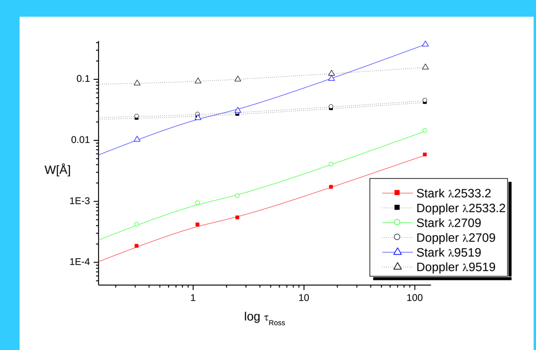

Fig. 3. Stark and Doppler broadening for spectral lines λ2533.2, λ2709, and λ9519 as a function of optical depth, but for the atmosphere of A-type star (Majlinger et al, 2020a) with model parameters log g = 4.5 and Teff = 10000 K (Kurucz,1979).

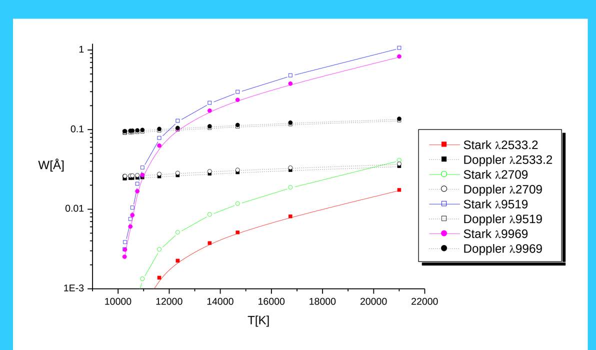

Fig. 4. Stark and Doppler broadening for spectral lines λ2533.2, λ2709, λ9519 and λ9969 optical depth in the atmosphere of DA white dwarf as a function of atmospheric layer temperature instead of optical depth (Majlinger et al, 2020b). Simulation is done with choice of model parameters, T_{eff} = 15000 K and log g = 8 (Wickramarsinghe, 1972).

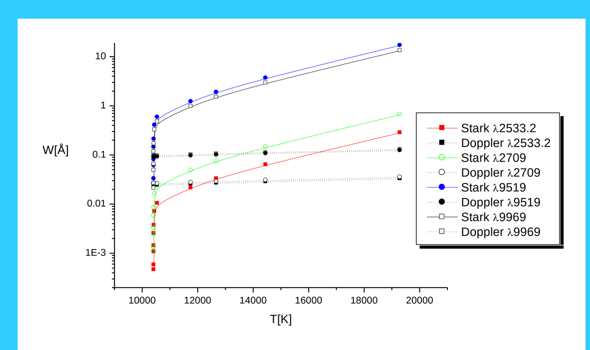

Fig. 5. Stark and Doppler broadening for spectral lines λ2533.2, λ2709, λ9519 and λ9969 optical depth in the atmosphere of DB white dwarf as a function of atmospheric layer temperature instead of optical depth (Majlinger et al, 2020b).. Simulation is done with choice of parameters T_{eff} = 15000 K and log g = 8 (Wickramarsinghe, 1972).

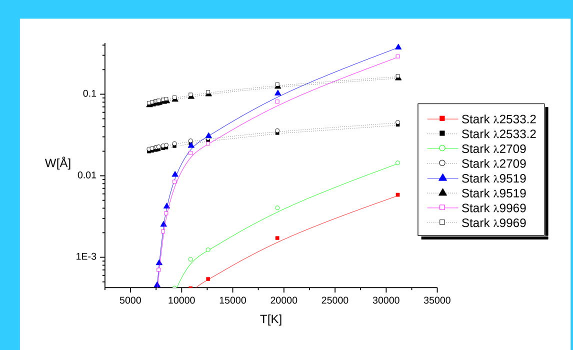

Stark and Doppler broadening for spectral lines λ2533.2, λ2709, λ9519 and λ9969 as a function of atmospheric layer temperature instead of optical depth for the atmosphere of A-type star (Majlinger et al, 2020b) with parameters log g = 4.5 and Teff = 10000 K (Kurucz,1979).

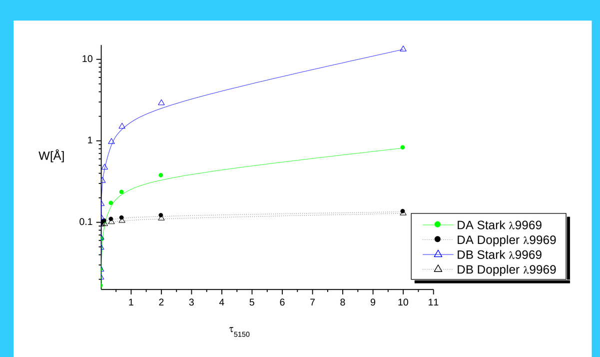

Fig. 7. Comparison of Stark and Doppler broadening influence on Co II line λ9969 in the atmosphere of DA and DB white dwarf respectively, as a function of optical depth (Majlinger et al, 2020b). Simulation is done with choice of parameters T_{eff} = 15000 K and log g = 8 (Wickramarsinghe, 1972).

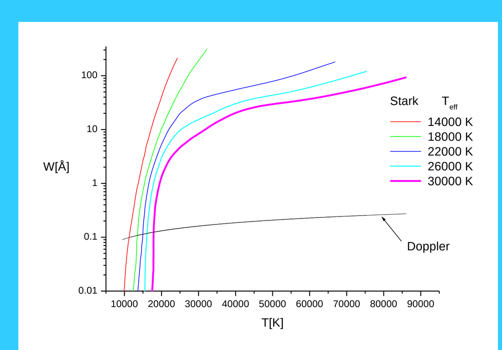

Fig. 8. Stark and Doppler broadening of Co II spectral line λ9969 as a function of temperature of atmospheric layers in DB white dwarf (Majlinger et al, 2020b). Stark widths are shown for five different values of effective temperature, T_{eff} = 14000 – 30000 K, log g = 8. (Koester, 1980).

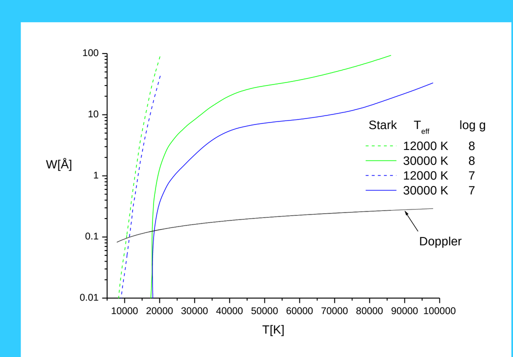

Fig. 9. Stark and Doppler broadening of Co II line λ9969 as a function of temperature of atmospheric layers in DB white dwarf (Majlinger et al, 2020b) for two different values of model gravity, log g = 7 and log g = 8, each with two extremal values of effective temperature, T_{eff} = 12000 K and T_{eff} = 30000 K (Koester, 1980).

Tab. 1. MSE Stark FWHM (W_{MSE}) calculated for Co II transitions for five different temperature values. Electron density is 10^{23} m^{-3} (Majlinger et al, 2020a).

Transitions	λ (Å)	W_{MSE}(Å)				
T(K)		5000	10000	20000	50000	100000
$(^2G)4sa\,^3G-(^2G)4py\,^3F^o$	2370.0	0.5026E-01	0.3554E-01	0.2513E-01	0.1589E-01	0.1144E-01
$(^2G)4sa\,^3G-(^2G)4py\,^3G^o$	2326.8	0.5299E-01	0.3747E-01	0.2650E-01	0.1676E-01	0.1207E-01
$(^2G)4sa\,^3G-(^2G)4py\,^3H^o$	2404.1	0.6027E-01	0.4262E-01	0.3013E-01	0.1906E-01	0.1381E-01
$(^2G)4sb\,^1G-(^2G)4py\,^1F^o$	2446.8	0.5557E-01	0.3929E-01	0.2778E-01	0.1757E-01	0.1269E-01
$(^2G)4sb\,^1G-(^2G)4py\,^1G^o$	2547.5	0.6506E-01	0.4600E-01	0.3253E-01	0.2057E-01	0.1497E-01
$(^2G)4sb\,^1G-(^2G)4py\,^1H^o$	2511.9	0.6818E-01	0.4821E-01	0.3409E-01	0.2156E-01	0.1571E-01
$(^2D2)4sb\,^1D-(^2D2)4py\,^1P^o$	2308.2	0.4696E-01	0.3321E-01	0.2348E-01	0.1485E-01	0.1065E-01
$(^2D2)4sb\,^1D-(^2D2)4py\,^1D^o$	2412.3	0.5872E-01	0.4152E-01	0.2936E-01	0.1857E-01	0.1343E-01
$(^2D2)4sb\,^1D-(^2D2)4py\,^1F^o$	2419.2	0.6714E-01	0.4747E-01	0.3357E-01	0.2123E-01	0.1543E-01
$(^2D2)4sa\,^3D-(^2D2)4px\,^3P^o$	2251.8	0.4312E-01	0.3049E-01	0.2156E-01	0.1364E-01	0.9756E-02
$(^2D2)4sa\,^3D-(^2D2)4pw\,^3D^o$	2424.0	0.5676E-01	0.4014E-01	0.2838E-01	0.1795E-01	0.1298E-01
$(^2D2)4sa\,^3D-(^2D2)4px\,^3F^o$	2360.4	0.6158E-01	0.4354E-01	0.3079E-01	0.1947E-01	0.1410E-01
$(^4P)4sb\,^5P-(^4P)4pz\,^5S^o$	2613.4	0.5369E-01	0.3797E-01	0.2685E-01	0.1698E-01	0.1220E-01
$(^4P)4sb\,^5P-(^4P)4py\,^5D^o$	2533.2	0.8066E-01	0.5704E-01	0.4033E-01	0.2551E-01	0.1871E-01
$(^4P)4sb\,^5P-(^4P)4py\,^5P^o$	2435.9	0.6031E-01	0.4265E-01	0.3016E-01	0.1907E-01	0.1381E-01
$(^2P)4sc\,^3P-(^2P)4px\,^3P^o$	2496.6	0.5972E-01	0.4223E-01	0.2986E-01	0.1889E-01	0.1371E-01
$(^2P)4sc\,^3P-(^2P)4px\,^3D^o$	2348.3	0.6622E-01	0.4682E-01	0.3311E-01	0.2094E-01	0.1519E-01
$(^2P)4sc\,^3P-(^2P)4py\,^3S^o$	2215.9	0.3987E-01	0.2819E-01	0.1993E-01	0.1261E-01	0.9018E-02
$(^2P)4sa\,^1P-(^2P)4px\,^1D^o$	2523.7	0.7837E-01	0.5542E-01	0.3919E-01	0.2478E-01	0.1817E-01
$(^2P)4sa\,^1P-(^2P)4p\,^1S^o$	2479.8	0.7578E-01	0.5359E-01	0.3789E-01	0.2396E-01	0.1752E-01
$(^2P)4sa\,^1P-(^2P)4px\,^1P^o$	2311.0	0.5362E-01	0.3792E-01	0.2681E-01	0.1696E-01	0.1221E-01
$(^2H)4sa\,^3H-(^2H)4px\,^3G^o$	2423.0	0.5287E-01	0.3739E-01	0.2644E-01	0.1672E-01	0.1204E-01
$(^2H)4sa\,^3H-(^2H)4px\,^3I^o$	2431.3	0.6054E-01	0.4281E-01	0.3027E-01	0.1914E-01	0.1388E-01
$(^2H)4sa\,^3H-(^2H)4py\,^3H^o$	2261.2	0.5030E-01	0.3556E-01	0.2515E-01	0.1591E-01	0.1143E-01
$(^2H)4sa\,^1H-(^2H)4py\,^1G^o$	2348.5	0.5224E-01	0.3694E-01	0.2612E-01	0.1652E-01	0.1189E-01
$(^2H)4sa\,^1H-(^2H)4py\,^1H^o$	2282.6	0.5330E-01	0.3769E-01	0.2665E-01	0.1686E-01	0.1213E-01
$(^4F)4sa\,^5F-(^4F)4px\,^5F^o$	2406.2	0.5523E-01	0.3905E-01	0.2762E-01	0.1747E-01	0.1262E-01
$(^4F)4sa\,^5F-(^4F)4px\,^5D^o$	2333.1	0.5083E-01	0.3594E-01	0.2541E-01	0.1607E-01	0.1157E-01
$(^4F)4sa\,^5F-(^4F)4px\,^5G^o$	2301.6	0.5212E-01	0.3685E-01	0.2606E-01	0.1648E-01	0.1186E-01
$(^4F)5se\,^5F-(^4F)5p\,^5G^o$	8223.5	3.185	2.252	1.593	1.201	1.196
$(^4F)4sa\,^5F-(^4F)5p\,^5G^o$	1079.4	0.3461E-01	0.2448E-01	0.1731E-01	0.1266E-01	0.11418E-1
$(^4F)4px\,^5F^o-(^4F)5s\,^5F$	2569.4	0.1395	0.9865E-01	0.6975E-01	0.4989E-01	0.4414E-01
$(^4F)4px\,^5D^o-(^4F)5s\,^5F$	2658.2	0.1451	0.1026	0.7257E-01	0.5208E-01	0.4622E-01
$(^4F)4px\,^5G^o-(^4F)5s\,^5F$	2700.3	0.1597	0.1129	0.7984E-01	0.5688E-01	0.5000E-01
$(^4F)4sb\,^3F-(^4F)4p\,^3D^o$	2581.8	0.5177E-01	0.3661E-01	0.2589E-01	0.1637E-01	0.1176E-01
$(^4F)4sb\,^3F-(^4F)4p\,^3F^o$	2516.1	0.6499E-01	0.4596E-01	0.3250E-01	0.2055E-01	0.1493E-01
$(^4F)4sb\,^3F-(^4F)4p\,^3G^o$	2408.8	0.5399E-01	0.3817E-01	0.2699E-01	0.1707E-01	0.1230E-01
$(^4F)5se\,^3F-(^4F)5p\,^5D^o$	10624	4.292	3.035	2.170	1.670	1.660
$(^4F)5se\,^3F-(^4F)5p\,^5F^o$	9969	4.479	3.167	2.251	1.780	1.768
$(^4F)5se\,^3F-(^4F)5p\,^5G^o$	9519	4.586	3.243	2.293	1.844	1.789
$(^4F)4sb\,^3F-(^4F)5p\,^3G^o$	1148.5	0.4642E-01	0.3297E-01	0.2331E-01	0.1776E-01	0.1759E-01
$(^4F)4sb\,^3F-(^4F)5p\,^3F^o$	1145.8	0.4291E-01	0.3034E-01	0.2146E-01	0.1636E-01	0.1602E-01
$(^4F)4sb\,^3F-(^4F)5p\,^3D^o$	1144.7	0.3782E-01	0.2675E-01	0.1891E-01	0.1422E-01	0.1388E-01
$(^4F)4px\,^3G^o-(^4F)5se\,^3F$	2709.0	0.1852	0.1310	0.9262E-01	0.6718E-01	0.6041E-01
$(^4F)4px\,^3F^o-(^4F)5se\,^3F$	2785.4	0.1709	0.1209	0.8545E-01	0.6087E-01	0.5391E-01
$(^4F)4px\,^3D^o-(^4F)5se\,^3F$	2929.8	0.1627	0.1151	0.8136E-01	0.5676E-01	0.4920E-01

Tab 2. Calculated values of Stark widths from Tab. 1 are used to find approximative formula of their dependence on temperature (Sahal-Bréchot et al. 2011):

$$\log w(T) = a + b\log T + c\log^2 T$$

Coefficients *a*, *b* and *c* are tabulated here (Majlinger et al, 2020a).

Transitions	λ(Å)	a	b	c
$(^2G)4sa\,^3G-(^2G)4py\,^3F^o$	2370.0	1.59957	−0.99996	0.05902
$(^2G)4sa\,^3G-(^2G)4py\,^3G^o$	2326.8	1.71162	−1.04240	0.06403
$(^2G)4sa\,^3G-(^2G)4py\,^3H^o$	2404.1	1.84208	−1.07850	0.06837
$(^2G)4sb\,^1G-(^2G)4py\,^1F^o$	2446.8	1.73637	−1.04462	0.06433
$(^2G)4sb\,^1G-(^2G)4py\,^1G^o$	2547.5	1.93042	−1.10520	0.07158
$(^2G)4sb\,^1G-(^2G)4py\,^1H^o$	2511.9	2.01712	−1.13688	0.07533
$(^2D2)4sb\,^1D-(^2D2)4py\,^1P^o$	2308.2	1.60236	−1.01483	0.06071
$(^2D2)4sb\,^1D-(^2D2)4py\,^1D^o$	2412.3	1.82946	−1.07766	0.06824
$(^2D2)4sb\,^1D-(^2D2)4py\,^1F^o$	2419.2	2.00560	−1.13425	0.07497
$(^2D2)4sa\,^3D-(^2D2)4px\,^3P^o$	2251.8	1.48404	−0.97603	0.05612
$(^2D2)4sa\,^3D-(^2D2)4pw\,^3D^o$	2424.0	1.74483	−1.04446	0.06434
$(^2D2)4sa\,^3D-(^2D2)4px\,^3F^o$	2360.4	1.89552	−1.09933	0.07080
$(^4P)4sb\,^5P-(^4P)4pz\,^5S^o$	2613.4	1.52274	−0.94973	0.05310
$(^4P)4sb\,^5P-(^4P)4py\,^5D^o$	2533.2	2.25081	−1.21401	0.08450
$(^4P)4sb\,^5P-(^4P)4py\,^5P^o$	2435.9	1.86806	−1.09060	0.06978
$(^2P)4sc\,^3P-(^2P)4px\,^3P^o$	2496.6	1.79819	−1.05986	0.06622
$(^2P)4sc\,^3P-(^2P)4px\,^3D^o$	2348.3	1.99068	−1.12977	0.07441
$(^2P)4sc\,^3P-(^2P)4py\,^3S^o$	2215.9	1.43500	−0.96884	0.05526
$(^2P)4sa\,^1P-(^2P)4px\,^1D^o$	2523.7	2.20154	−1.19647	0.08243
$(^2P)4sa\,^1P-(^2P)4p\,^1S^o$	2479.8	2.15636	−1.18157	0.08063
$(^2P)4sa\,^1P-(^2P)4px\,^1P^o$	2311.0	1.76736	−1.06636	0.06684
$(^2H)4sa\,^3H-(^2H)4px\,^3G^o$	2423.0	1.63534	−1.00682	0.05988
$(^2H)4sa\,^3H-(^2H)4px\,^3I^o$	2431.3	1.84304	−1.07808	0.06832
$(^2H)4sa\,^3H-(^2H)4py\,^3H^o$	2261.2	1.69006	−1.04262	0.06402
$(^2H)4sa\,^1H-(^2H)4py\,^1G^o$	2348.5	1.70875	−1.04383	0.06418
$(^2H)4sa\,^1H-(^2H)4py\,^1H^o$	2282.6	1.79317	−1.07979	0.06841
$(^4F)4sa\,^5F-(^4F)4px\,^5F^o$	2406.2	1.70341	−1.03041	0.06268
$(^4F)4sa\,^5F-(^4F)4px\,^5D^o$	2333.1	1.63779	−1.01577	0.06088
$(^4F)4sa\,^5F-(^4F)4px\,^5G^o$	2301.6	1.69809	−1.03922	0.06363
$(^4F)5se\,^5F-(^4F)5p\,^5G^o$	8223.5	6.17653	−2.41088	0.23770
$(^4F)4sa\,^5F-(^4F)5p\,^5G^o$	1079.4	2.01187	−1.34472	0.10949
$(^4F)4px\,^5F^o-(^4F)5s\,^5F$	2569.4	4.17608	−2.07526	0.19401
$(^4F)4px\,^5D^o-(^4F)5s\,^5F$	2658.2	4.21517	−2.08719	0.19562
$(^4F)4px\,^5G^o-(^4F)5s\,^5F$	2700.3	4.20460	−2.05891	0.19181
$(^4F)4sb\,^3F-(^4F)4p\,^3D^o$	2581.8	1.51781	−0.95483	0.05369
$(^4F)4sb\,^3F-(^4F)4p\,^3F^o$	2516.1	1.95524	−1.11699	0.07293
$(^4F)4sb\,^3F-(^4F)4p\,^3G^o$	2408.8	1.73277	−1.04855	0.06475
$(^4F)5se\,^3F-(^4F)5p\,^5D^o$	10624	6.22399	−2.38153	0.23564
$(^4F)5se\,^3F-(^4F)5p\,^5F^o$	9969	6.09300	−2.31637	0.22877
$(^4F)5se\,^3F-(^4F)5p\,^5G^o$	9519	6.00299	−2.27062	0.22365
$(^4F)4sb\,^3F-(^4F)5p\,^3G^o$	1148.5	4.22723	−2.35867	0.23189
$(^4F)4sb\,^3F-(^4F)5p\,^3F^o$	1145.8	4.16586	−2.34544	0.23017
$(^4F)4sb\,^3F-(^4F)5p\,^3D^o$	1144.7	4.18926	−2.37799	0.23336
$(^4F)4px\,^3G^o-(^4F)5se\,^3F$	2709.0	4.43387	−2.14589	0.20324
$(^4F)4px\,^3F^o-(^4F)5se\,^3F$	2785.4	4.34314	−2.11157	0.19813
$(^4F)4px\,^3D^o-(^4F)5se\,^3F$	2929.8	4.26085	−2.07376	0.19245

Discussion of results and conclusion

A) Stark broadening over Doppler broadening is more significant for the atmosphere of DA and DB WD than for A-type star beacuse of higher electron density (especially for DB WD where helium-rich atmosphere produces more electrons than hydrogen-rich DA atmosphere)

B) Stark width is more significant for lines from infrared than for ultraviolet part of spectrum (Doppler width rises with λ, while Stark width rises with λ^2) beacuse for higher wavelenght corresponding atomic energy levels are closer and perturbation of radiators is greater, so emmited/absorbed line is broader

C) Last line, Co II λ9959, is an exception, beacuse corresponding energy levels for this line are further away, so the perturbation is smaller

D) In the atmosphere of DB WD, Stark broadening becomes more prominent with rising of T_{eff} and log g (higher T_{eff} produces more ionized helium and higher gravity increases electron density)

Acknowledgments

This work was supported by the Astronomical Observatory Belgrade and Institute of Physics Belgrade, through the grant by the Ministry of Education, Science, and Technological Development of the Republic of Serbia.

References

Dimitrijević, M. S., Konjević, N.: 1980, *J. Quant. Spectrosc. Radiat. Transfer*, **24**, 454.

Koester, D., 1980, *Astron. Astrophys. Soppl. Ser.*, **39**, 401

Kurucz, R. L., 1979, *Astrophys. J. Suppl. Series*, **40**,1

Majlinger, Z., Dimitrijević, M. S., Simić, Z., 2018, *Astron. Astrophys. Trans.*, **30(3)**, 323.

Majlinger, Z., Dimitrijević, M. S., Srećković, V. A.: 2020a, *MNRAS*, **496**, 5584.

Majlinger, Z., Dimitrijević, M. S., Srećković, V. A.: 2020b, *Data*, accepted.

Sahal-Bréchot, S., Dimitrijević, M.S., and Ben Nessib, N., 2011, *Baltic Astron.*, **20**, 523.

Wickramarsinghe, D. T., 1972, *Mem. R. Astron. Soc.*, **76**, 129